IJSES
Volume 9, Issue 8, pp. 26-35, 2025.
International Journal of Scientific Engineering and Science
ISSN (Online): 2456-7361

Spatial Distribution of Natural Radioactivity in the Volcanic Soil of Antsiranana II District, Madagascar

TSILAILAY Astellinah Née Stevenah[1], DONNE Zafizara[1], RANDRIANANTENAINA Fanjanirina Rovatiana[2], SOLONJARA Asivelo Fanantenansoa[2], ASIMANANA Frédéric[1]
[1]Department of Nuclear Metrology and Environment, Faculty of Science, University of Antsiranana, Madagascar
[2]Department of Nuclear Techniques and Analysis, National Institute of Sciences and Nuclear Techniques, Madagascar

Abstract— *The study shows the first comprehensive radiological characterization of the soils in the district of Antsiranana II, a volcanic region in northern Madagascar that was not previously documented. A total of 23 soil samples, representative of the geo-pedological diversity of the district, were collected and analyzed by gamma spectrometry with NaI(Tl) detector. The mean activity concentrations for ^{40}K, ^{238}U, and ^{232}Th were measured at 194 ± 83 Bq.kg^{-1}, 48 ± 19 Bq.kg^{-1}, and 61 ± 18 Bq.kg^{-1}, respectively. While the ^{40}K levels are significantly lower than the world average, the concentrations of ^{238}U and ^{232}Th are 1.4 and 2.0 times higher, respectively, revealing a distinct geochemical signature linked to the local volcanic geology. The spatial analysis highlights a heterogeneous distribution governed by a combination of factors: the ^{40}K content is mainly controlled by altitude and the nature of the volcanic rocks (evolved vs. mafic); the distribution of ^{232}Th, which is geochemically immobile, is a faithful tracer of the primary lithology; whereas that of ^{238}U, which is more mobile, is influenced by both the parent rock and secondary redistribution processes. This study provides a reference database for environmental monitoring, geological studies, and land management in the region.*

Keywords—*Natural Radioactivity, Volcanic Soil, Gamma Spectrometry, Spatial Distribution, Antsiranana II.*

I. INTRODUCTION

Natural radioactivity is a ubiquitous component of the terrestrial environment, originating from primordial radionuclides such as potassium-40 (^{40}K) and the decay chains of uranium-238 (^{238}U) and thorium-232 (^{232}Th). The distribution of these radionuclides in the soil is closely linked to the geology of the parent rock as well as the pedological processes that govern soil formation and alteration (UNSCEAR, 2000; Tzortzis *et al.*, 2003; Rabesiranana, 2017; Barijaona *et al.*, 2017; Donné *et al.*, 2021; Anguma et al., 2023; Demewoz *et al.*, 2025; Djaovagnono *et al.*, 2025). Establishing reference data on soil radioactivity is therefore fundamental. It allows for the assessment of population and environmental exposure to ionizing radiation, provides a baseline for monitoring potential contamination, and deepens the understanding of regional geochemical characteristics (Demewoz *et al.*, 2025; López-Pérez *et al.*, 2021; Ngoko *et al.*, 2024; Ngoko *et al.*, 2025).

Madagascar, with its complex and diverse geology, presents a unique context for such studies. However, many regions of the country remain uncharacterized from a radiological standpoint. The DIANA region, located in the north of the island, and particularly the district of Antsiranana II, is one such area. The population of this district is predominantly rural, and its livelihood depends heavily on agriculture, implying a close and continuous interaction with the soil. Although environmental radioactivity studies have been conducted in some communes of the district, such as the rural commune of Ramena (Kall *et al.*, 2014), the rural commune of Mangaoko, and that of Andranovondronina (Rakotonarivo *et al.*, 2019), and the rural commune of Joffre-Ville (Donné *et al.*, 2021), their geographical coverage remains partial and does not reflect the diversity of the entire territory.

The present work therefore aims to fill this gap by conducting an exhaustive radiological characterization to establish a representative reference database for the entire district.

The specific objectives of this study are: (1) to quantify the activity concentrations of ^{40}K, ^{238}U, and ^{232}Th in the soils; (2) to analyze the influence of geo-pedological characteristics and altitude on the distribution of these radionuclides; (3) to study the statistical correlations between their activity concentrations; and (4) to develop spatial distribution maps to identify geographical variations and potential radiological anomalies.

II. MATERIAL AND METHODS

2.1. Description and Geology of the Study Area

The study was conducted in the district of Antsiranana II, an administrative subdivision of the DIANA region, located at the northern tip of Madagascar. The district lies between the geographical coordinates 11°55'25.60" and 12°51'52.60" South latitude, and between 48°43'33.84" and 49°37'19.95" East longitude (Fig. 1). The District of Antsiranana II covers an area of 5,645 km². According to the 2009 administrative division, this district is composed of 21 rural communes, but currently, it comprises 23 rural communes, including Andrafiabe, Andranofanjava, Andranovondronina, Anivorano-Nord, Antsoha, Antsakoabe, Ankarongana, Anketrakabe, Antsahampano, Antsalaka, Bobasakoa, Joffre-Ville, Mahalina, Mahavanona, Mangaoko, Morarano (Ex-Mosorolava), Ramena, Sadjoavato, Sakaramy, Antanamitarana, Ambondrona, Bobakilandy, and Ambolobozobe (CREAM, 2013).

Its territory is marked by an exceptional geological and topographical context, dominated by the volcanic massif of the Amber Mountain. The latter presents as a vast volcanic cone culminating at over 1400 meters, from which a dense and

International Journal of Scientific Engineering and Science
Volume 9, Issue 8, pp. 26-35, 2025. ISSN (Online): 2456-7361

torrential hydrographic network radiates (Ségalen, 1956). Around this mountainous core, the relief is organized into vast plateaus resulting from the erosion of ancient lava flows, while the periphery is marked by sedimentary massifs with steep cliffs (e.g., Montagne des Français) and alluvial plains formed by river deposits, such as the Rodo.

The geology of the district reflects a complex history dominated by a duality between an ancient sedimentary basement, spanning from the Jurassic to the Eocene, and a recent volcanic cover from the Neogene to the Quaternary, which directly conditions soil formation. The base consists of a major Mesozoic and Cenozoic sedimentary succession, testifying to an alternation of marine and continental depositional environments. It comprises a diverse Cretaceous sequence, including marls and sandstones (Saharena Formation), as well as marine limestones and continental sandstones from the Lower Jurassic (Isalo I) and Middle to Upper Jurassic periods, as well as hard Eocene limestones with Nummulites (Besairie, 1970; Lemoine, 1906). These sedimentary formations, which today outcrop mainly on the periphery of the district, have been profoundly reworked and covered by intense volcanic activity. This episode, which likely began in the Middle Miocene (Cucciniello *et al.*, 2011; Donné *et al.*, 2021), gave rise to the Amber Mountain massif, an immense stratovolcano of 2,500 km² formed by a complex assembly of lava flows, volcanic necks, scoria cones, and pyroclastic deposits. Petrologically, the volcanic rocks, which cover more than two-thirds of the region, are heterogeneous, mostly basic (alkaline basalts, basanites, tephrites), although more acidic rocks (trachytes, phonolites, rhyolites) are present but localized (Barat, 1958; Ségalen, 1956). These volcanic formations rest unconformably on the sedimentary strata. The most recent deposits are of Quaternary origin and are concentrated along the coast, including alluvium, mangrove muds, as well as dunes and sands of dunal origin, particularly on the East coast (Ségalen, 1956).

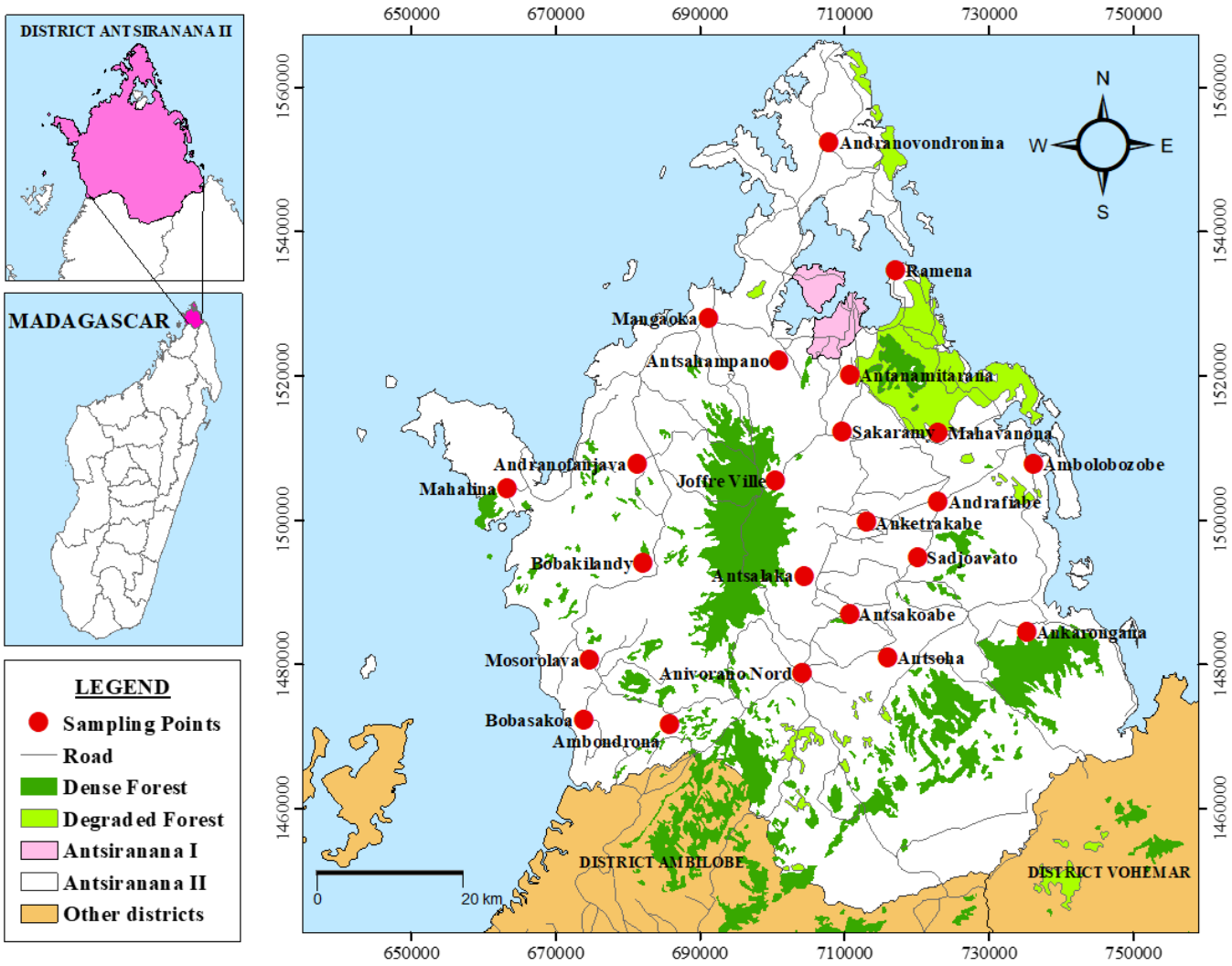

Fig. 1. Location of sampling points

The pedological structure is a direct reflection of this diversity of parent rocks and a marked climatic gradient, with a very humid climate at the summit of the massif and drier on the periphery (Ségalen, 1956). This results in a mosaic of soils. Among the developed and deep soils, we distinguish ferralitic and lateritic soils, formed under the cool and rainy climate of

the Amber Mountain on volcanic rocks. They are acidic and are subdivided into typical soils (brown-yellow or red) on medium slopes and humic soils, very rich in organic matter, at high altitudes. The drier periphery is characterized by complexes of tropical ferruginous soils and less-developed Mediterranean red soils, which develop on a wide variety of parent rocks (basalt, sandstone, limestone, sand). To these are added calcimorphic soils (brown calcareous soils, rendzinas), influenced by limestone. The poorly or undeveloped soils include alluvial soils (valley alluvium, coastal dune sands) and a complex of lithosols and skeletal soils directly linked to the parent rock on recent lava flows or steep slopes.

From a demographic perspective, the district's population represented 14.5% of the total population of the DIANA Region, mostly distributed in rural areas (CREAM, 2013).

2.2. Sample Collection and Preparation

Sampling campaigns were conducted during the month of July 2024. A total of 23 soil samples were collected, covering all 23 rural communes of the Antsiranana II district, to ensure maximum representativeness of the geological and pedological diversity of the territory. The sampling points were selected to reflect areas of interest for the local population, including village areas and agricultural lands (rice paddies and other crops), where the interaction between humans and the soil is most intense.

The geolocation of each sampling point was recorded using a GPS (Global Positioning System) receiver. The coordinate data were then integrated into ArcGIS 10.5 software to create spatial distribution maps (Fig. 1), using base maps from the FTM (Foiben-Taosarintanin'i Madagasikara) projected in the Laborde system.

At each site, a composite sample of approximately 500 g was collected from a surface area of about 1 m² at a depth of 30 cm. The samples were taken from undisturbed areas, after carefully removing the surface litter (dead leaves, plant debris) to access the intact soil horizon. Each sample was placed in a plastic bag, labeled with a unique code from ANTII-1 to ANTII-23, where the prefix "ANTII" designates the study district of Antsiranana II.

At the laboratory of the National Institute of Nuclear Sciences and Techniques (INSTN) in Antananarivo, the samples were prepared according to a standardized protocol. This protocol consisted of: (1) drying the samples in an oven at 105 °C until a constant weight was obtained; (2) grinding and sieving through a 2 mm mesh to obtain a fine and homogeneous powder; (3) packing this powder into cylindrical polyethylene containers (volume of 200 cm³), which were hermetically sealed. These containers were stored for a minimum period of four weeks before analysis to ensure the establishment of secular equilibrium between ^{226}Ra (a descendant of ^{238}U) and ^{228}Ra (a descendant of ^{232}Th) with their respective short-lived gamma-emitting descendants.

2.3. Gamma-ray Spectrometry and Determination of Specific Activities

The specific activities of the natural radionuclides were measured using a high-sensitivity gamma spectrometer. The detection system consists of a 3" x 3" thallium-doped sodium iodide (NaI(Tl)) scintillation detector (ORTEC, Model 905-4), coupled to a multichannel analyzer. To reduce the influence of cosmic and terrestrial background radiation, the detector is housed in a 10 cm thick lead shield.

The energy and efficiency calibration of the spectrometer was performed using the same containers and geometry as for the samples. Certified reference materials from the International Atomic Energy Agency (IAEA) were used: RGK-1 (for Potassium), RGU-1 (for Uranium), and RGTh-1 (for Thorium).

The specific activity of ^{40}K was determined directly from its gamma emission peak at 1461 keV. The activities of ^{238}U and ^{232}Th were evaluated assuming secular equilibrium within their respective decay chains. The activity of ^{238}U was deduced from the gamma peak at 1764.5 keV emitted by ^{214}Bi, and that of ^{232}Th from the peak at 2614.5 keV emitted by ^{208}Tl (Chiozzi *et al.*, 2000; Chiozzi *et al*., 2001; Cinelli *et al*., 2016; Stolerie *et al.,* 2021; Rahelivao *et al*., 2023; Ngoko *et al*., 2024; Djaovagnono *et al*., 2025). For each sample, the acquisition time was set to 12 hours (43200 s) to obtain robust counting statistics and minimize statistical uncertainties.

The calculation of the specific activities of the radionuclides was determined using the spectral window analysis method, as described by Rybach (1988) and Chiozzi *et al*. (2000). This method is based on the proportionality between the net count rate $R_{i,j}$ in three energy windows (i = K, U, Th) and the activities of the corresponding $A_{n,j}$. The system of equations is as follows (Chiozzi *et al.,* 2000; Stolerie *et al.,* 2021; Djaovagnono *et al.,* 2025):

$$R_{i,j} = \sum_{n=1}^{3} \varepsilon_{i,n} \times A_{n,j} \qquad (1)$$

Where the indices *i*, *j*, and *n* (ranging from 1 to 3) represents the regions of interest (K, U, Th), the standards (RGK-1, RGU-1, and RGTh-1), and the radionuclide (^{40}K, ^{238}U, ^{232}Th), respectively; $\varepsilon_{i,n}$ is the detection efficiency in the *i*-th ROI for the *n*-th radionuclide. The net count rate is given by:

$$R_{i,j} = \frac{N_{i,j}}{t_j} - B_i \qquad (2)$$

Where $N_{i,j}$ is the number of recorded counts in ROI *i* for the standard *j*; t_j is the counting time for standard *j*; and B_i is the background count rate in the *i*-th ROI.

Thus, the equation (1) allows for the construction of an efficiency matrix (*E*) that links the net count rates in each window to the actual activities of the radionuclides. The link between the measured net count rates (*R*) and the radionuclide activities (*A*) in a soil sample is described by the following matrix relation (Chiozzi *et al*., 2000; Stolerie *et al.,* 2021; Djaovagnono *et al*., 2025):

$$\begin{bmatrix} R_K \\ R_U \\ R_{Th} \end{bmatrix} = \begin{bmatrix} \varepsilon_{1,1} & \varepsilon_{1,2} & \varepsilon_{1,3} \\ 0 & \varepsilon_{2,2} & \varepsilon_{2,3} \\ 0 & \varepsilon_{3,2} & \varepsilon_{3,3} \end{bmatrix} \begin{bmatrix} A_K \\ A_U \\ A_{Th} \end{bmatrix} \qquad (3)$$

International Journal of Scientific Engineering and Science
Volume 9, Issue 8, pp. 26-35, 2025. ISSN (Online): 2456-7361

Where R is the vector of net count rates (R_K , R_U , R_{Th}) ; E is the efficiency matrix (3 x 3) determined during calibration, and A is the vector of unknown activities (A_K , A_U , A_{Th}).

To determine the activities in a sample, the equation is inverted:

$$\begin{bmatrix} A_K \\ A_U \\ A_{Th} \end{bmatrix} = \begin{bmatrix} a_{1,1} & a_{1,2} & a_{1,3} \\ 0 & a_{2,2} & a_{2,3} \\ 0 & a_{3,2} & a_{3,3} \end{bmatrix} \begin{bmatrix} R_K \\ R_U \\ R_{Th} \end{bmatrix} \quad (4)$$

This translates to the following system of equations, where the coefficients $a_{i,j}$ are the terms of the inverse matrix E^{-1} of E (Chiozzi *et al.*, 2000; Stolerie *et al.*, 2021; Djaovagnono *et al.*, 2025):

$$\begin{cases} A_K = a_{1,1}R_K + a_{1,2}R_U + a_{1,3}R_{Th} \\ A_U = a_{2,2}R_U + a_{2,3}R_{Th} \\ A_{Th} = a_{3,2}R_U + a_{3,3}R_{Th} \end{cases} \quad (5)$$

Knowing that the constants of the inverse matrix E^{-1} must be expressed as a function of the efficiency constants $\varepsilon_{i,n}$ in the three regions of interest.

The uncertainty on each activity is calculated by applying the law of error propagation. The general formula for the uncertainty of the radionuclide activity n is (Chiozzi *et al.*, 2000; Kall *et al.*, 2014; Stolerie *et al.*, 2021):

$$\sigma_{A_n} = \left(\sum_i \left[\left(R_i \times \sigma_{a_{n,i}} \right)^2 + \left(\alpha_{n,i} \times \sigma_{R_i} \right)^2 \right] \right)^{1/2} \quad (6)$$

Where σ_{A_n} is the final uncertainty on the calculated activity for radionuclide n; n is the index representing the radionuclide for which the activity is calculated (n = 1 for ^{40}K, n = 2 for ^{238}U, and n = 3 for ^{232}Th); i is the index representing each measurement window (i = 1 for the K window, i = 2 for the U window, i = 3 for the Th window); $\sum_i$ is the summation symbol indicating that the terms for all measurement windows i must be added; $a_{n,i}$ is the coefficient of the inverse matrix that links the activity n to the count rate i; R_i is the net count rate in the measurement window i; $\sigma_{a_{n,i}}$ is the uncertainty on the coefficient of the matrix $\alpha_{n,i}$; σ_{R_i} is the statistical uncertainty on the net count rate R_i .

III. Results and Discussion

3.1. Activity Concentrations of Natural Radionuclides

The results of the specific activity measurements of the radionuclides ^{40}K, ^{238}U series, and ^{232}Th series in the 23 soil samples from the district of Antsiranana II are presented in Table I and illustrated in Figures 2, 3, and 4.

The specific activity of ^{40}K ranges from 106 ± 10 Bq.kg^{-1} to 391 ± 16 Bq.kg^{-1}, with a mean value of 194 ± 83 Bq.kg^{-1}. This mean is significantly lower, by more than twofold, than the world average value of 400 Bq.kg^{-1} (UNSCEAR, 2000).

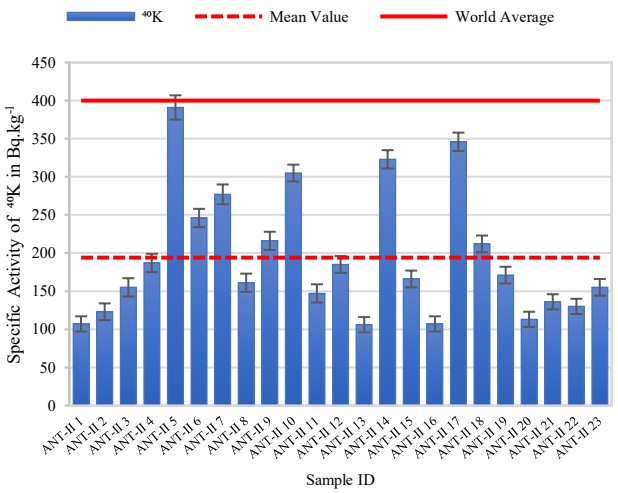

Fig. 2. Distribution of specific activities of ^{40}K

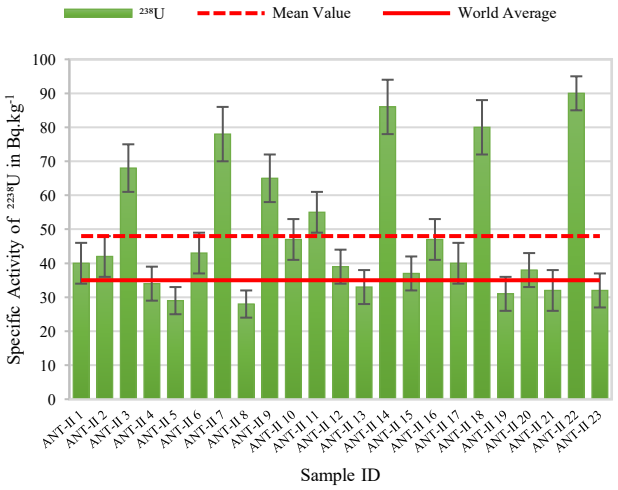

Fig. 3. Distribution of specific activities of ^{238}U

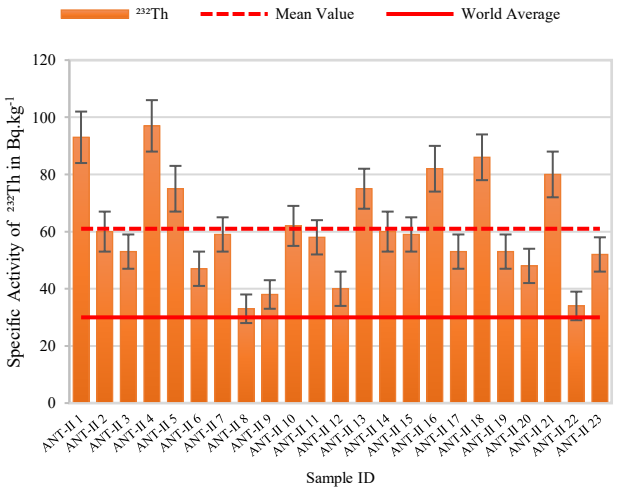

Fig. 4. Distribution of specific activities of ^{232}Th

International Journal of Scientific Engineering and Science
Volume 9, Issue 8, pp. 26-35, 2025. ISSN (Online): 2456-7361

TABLE I. Natural Radionuclide Activity in soil samples

Sample ID	Specific activity (Bq.kg^{-1})		
	^{40}K	^{238}U series	^{232}Th series
ANT-II 1	107 ± 10	40 ± 6	93 ± 9
ANT-II 2	123 ± 11	42 ± 6	60 ± 7
ANT-II 3	155 ± 12	68 ± 7	53 ± 6
ANT-II 4	187 ± 12	34 ± 5	97 ± 9
ANT-II 5	391 ± 16	29 ± 4	75 ± 8
ANT-II 6	246 ± 12	43 ± 6	47 ± 6
ANT-II 7	277 ± 13	78 ± 8	59 ± 6
ANT-II 8	161 ± 12	28 ± 4	33 ± 5
ANT-II 9	305 ± 12	65 ± 7	38 ± 5
ANT-II 10	147 ± 11	47 ± 6	62 ± 7
ANT-II 11	185 ± 12	55 ± 6	58 ± 6
ANT-II 12	180 ± 11	39 ± 5	40 ± 6
ANT-II 13	106 ± 10	33 ± 5	75 ± 7
ANT-II 14	323 ± 12	86 ± 8	60 ± 7
ANT-II 15	166 ± 11	37 ± 5	59 ± 6
ANT-II 16	107 ± 10	47 ± 6	82 ± 8
ANT-II 17	346 ± 12	40 ± 6	53 ± 6
ANT-II 18	212 ± 11	80 ± 8	86 ± 8
ANT-II 19	171 ± 11	31 ± 5	53 ± 6
ANT-II 20	113 ± 10	38 ± 5	48 ± 6
ANT-II 21	136 ± 10	50 ± 6	80 ± 8
ANT-II 22	130 ± 10	32 ± 5	34 ± 5
ANT-II 23	155 ± 11	32 ± 5	52 ± 6
Min	106	28	33
Max	391	86	97
Mean ± SD	194 ± 83	48 ± 19	61 ± 18
World Average (UNSCEAR, 2000)	400	35	30

This low potassium content is characteristic of the mafic volcanic rocks (basalts, basanites) that dominate the geology of the region, as these rocks are naturally poor in potassic minerals such as alkali feldspars. Concerning ^{238}U, the activity concentrations range from 28 ± 4 Bq.kg^{-1} to 86 ± 8 Bq.kg^{-1}, for a mean of 48 ± 19 Bq.kg^{-1}. This value is approximately 1.4 times higher than the world average of 35 Bq.kg^{-1}.

For ^{232}Th, the measured activities range from 33 ± 5 Bq.kg^{-1} to 97 ± 9 Bq.kg^{-1}, with a mean value of 61 ± 18 Bq.kg^{-1}. This concentration is twice as high as the world average of 30 Bq.kg^{-1} (UNSCEAR, 2000).

The analysis of the soils in the Antsiranana II district reveals a distinct radiological geochemical signature, characterized by a notable deficit in potassium (^{40}K) and a significant natural enrichment in actinides (^{238}U and ^{232}Th) compared to world averages. This profile is a direct consequence of the geological nature of the substratum, mainly composed of alkaline and mafic volcanic rocks that make up the Amber Mountain massif.

3.2. Statistical analysis of natural Radionuclide activities

The statistical analysis of the data, summarized in Table II and visualized in the box plots of Fig. 5, 6, and 7, provides additional information on the distribution of radionuclides.

For the three radionuclides, the mean value is higher than the median (^{40}K: 194 > 166; ^{238}U: 48 > 40; ^{232}Th: 61 > 59). This characteristic, coupled with positive skewness coefficients (1.02 for ^{40}K, 1.03 for ^{238}U, and 0.43 for ^{232}Th), indicates that the distributions are asymmetrical and skewed to the right. This suggests the presence of a few samples with abnormally high concentrations that pull the mean upwards.

TABLE II. Statistical distribution of natural radionuclide activities

Statistical parameters	^{40}K	^{238}U series	^{232}Th series
Minimum	106.00	28.00	33.00
Mode	107.00	32.00	53.00
Mean	194.13	48.43	60.74
Std. Error of Mean	17.28	4.06	3.79
Std. Deviation	82.85	19.47	18.19
25th percentile	130.00	33.00	48.00
50th percentile (Median)	166.00	40.00	59.00
75th percentile	246.00	65.00	75.00
Maximum	391.00	86.00	97.00
Skewness	1.02	1.03	0.43
Kurtosis	0.09	- 0.27	- 0.58
Test of Normality (Shapiro-Wilk)	<0.011	0.002	<0.290

The Shapiro-Wilk test for normality confirms this finding: the distributions of ^{40}K ($p < 0.05$) and ^{238}U ($p < 0.05$) concentrations do not follow a normal distribution. In contrast, the ^{232}Th distribution does not significantly deviate from a normal distribution ($p > 0.05$). The relatively high standard deviation for the three radionuclides (83 Bq.kg^{-1} for ^{40}K, 19 Bq.kg^{-1} for ^{238}U, and 18 Bq.kg^{-1} for ^{232}Th) indicates significant spatial heterogeneity of concentrations at the district level.

The statistical distribution of the radionuclides is heterogeneous and predominantly non-normal. The positive skewness, particularly marked for ^{40}K and ^{238}U, reveals the existence of localized radiological "hot spots" within the district, necessitating a more detailed spatial analysis to understand their origin.

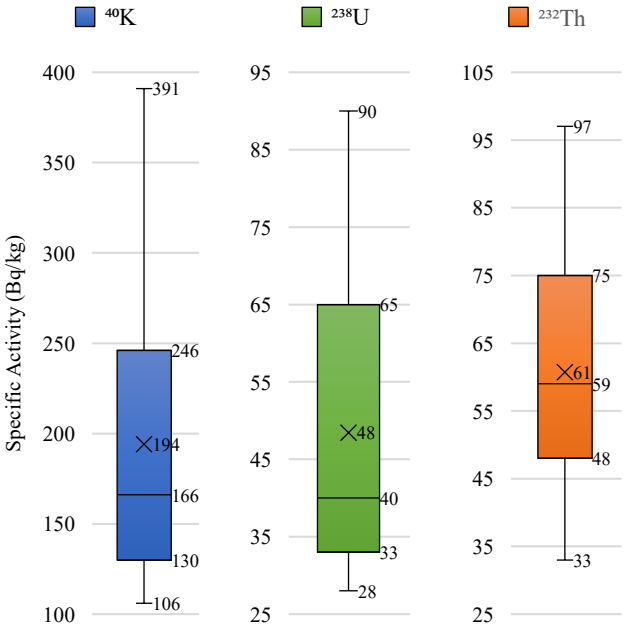

Fig. 5. Box plot of ^{40}K, ^{238}U, ^{232}Th Activities

To contextualize the obtained results and highlight the radiological specificities of the Antsiranana II district, a comparison was made with data from other studies conducted in Madagascar (Table III). This comparative analysis reveals distinct profiles, closely correlated with the geological nature of the different regions.

TABLE III. Comparison of similar study of natural radioactivity in soil samples from different localities of Madagascar

Locality	Average specific activity (Bq.kg^{-1})		
	^{40}K	^{238}U series	^{232}Th series
District of Antsiranana II	194	48	61
Rural Commune of Joffre-Ville (Donné *et al*., 2021)	218	44	90
Rural Commune of Ramena (Kall *et al*., 2014)	198	109	77
District of Ambilobe (Stolerie *et al.*, 2021)	518	18	40
District of Nosy-Be (Djaovagnono *et al*, 2025)	138	33	39
Ambanja city and its Surroundings (Rahelivao *et al*., 2023)	730	44	123
Ampasindava Peninsula, Ambanja (Rafidimanantsoa *et al*., 2021)	355	76	261
District of Antalaha (Ngoko *et al.,* 2024)	277	33	54
District of Fenoarivo Atsinanana (Randriamora *et al.,* 2017)	575	5390	21336
District of Befandriana Nord (Randrianarivo *et al.,* 2017)	200	21	198

The most relevant analysis concerns localities situated on the same Amber Mountain volcanic complex. The mean ^{40}K concentration (194 Bq.kg^{-1}) in the present study area is of the same order of magnitude as those measured in the rural commune of Joffre-Ville (218 Bq.kg^{-1}) and the rural commune of Ramena (198 Bq.kg^{-1}) (Donné *et al.,* 2021; Kall *et al.,* 2014). This consistency confirms the relative homogeneity of the potassic signature of the mafic volcanic rocks of the massif. However, divergences appear for the actinides. The mean value for ^{238}U (48 Bq.kg^{-1}) in the present study is similar to that of Joffre-Ville (44 Bq.kg^{-1}) but significantly lower than that of Ramena (109 Bq.kg^{-1}), while the concentration of ^{232}Th (61 Bq.kg^{-1}) is lower than in these two communes (90 and 77 Bq.kg^{-1}, respectively). These variations, although the sites share the same general volcanic substratum, could reflect local petrological differences or secondary redistribution processes of the elements.

Comparison with other volcanic regions of Madagascar, such as the district of Nosy-Be, reveals distinct profiles. The soils of Nosy-Be show systematically lower concentrations for all three radionuclides (138 Bq.kg^{-1} for ^{40}K, 33 Bq.kg^{-1} for ^{238}U, and 39 Bq.kg^{-1} for ^{232}Th), indicating that different volcanic provinces in Madagascar have their own geochemical signatures (Djaovagnono *et al*., 2025).

A marked contrast is observed with regions dominated by other geological formations. The district of Ambilobe, with a predominantly sedimentary substratum, shows an inverse profile: a very high ^{40}K content (518 Bq.kg^{-1}) but significantly lower concentrations of ^{238}U and ^{232}Th (18 Bq.kg^{-1} and 40 Bq.kg^{-1}) (Stolerie *et al*., 2021). Similarly, the soils of the Antalaha district show a higher ^{40}K concentration (277 Bq.kg^{-1}) and lower levels of ^{238}U and ^{232}Th (Ngoko *et al.,* 2024). These results clearly illustrate the primary influence of the parent rock on the radiological composition of soils.

Areas with complex geological contexts or known for their mineralized potential offer other points of comparison. The soils of Ambanja and its surroundings show extremely high concentrations of ^{40}K (730 Bq.kg^{-1}) and ^{232}Th (123 Bq.kg^{-1}), likely linked to granitic intrusions or metamorphic rocks, while having a ^{238}U content (44 Bq.kg^{-1}) surprisingly similar to our study area (Rahelivao et al., 2023). The district of Befandriana Nord, known for its heavy minerals, has a comparable ^{40}K content (200 Bq.kg^{-1}) but a ^{232}Th concentration (198 Bq.kg^{-1}) more than three times higher, which is consistent with an enrichment in thorium-bearing minerals like monazite (Randrianarivo *et al.,* 2017).

Finally, comparison with areas hosting proven deposits puts our results into perspective. The Ampasindava peninsula (Ambanja), with its rare earth element deposits, shows high concentrations of ^{238}U (76 Bq.kg^{-1}) and especially ^{232}Th (261 Bq.kg^{-1}) (Rafidimanantsoa *et al*., 2021). The case of the Fenoarivo Atsinanana district is extreme, with abnormally high values linked to monazite deposits (5390 Bq.kg^{-1} for ^{238}U and 21336 Bq.kg^{-1} for ^{232}Th) that are not representative of a geochemical background but of a mineralogical anomaly (Randriamora *et al*., 2017).

Indeed, this comparative analysis confirms that the Antsiranana II district has a distinctive radiological signature on a national scale. It is characterized by a notable potassium (^{40}K) deficit combined with a significant natural enrichment in uranium (^{238}U) and thorium (^{232}Th) compared to world averages. This signature is a direct imprint of the volcanic substratum, predominantly mafic and alkaline, of the Amber Mountain. This profile clearly distinguishes it from the sedimentary, granitic, or metamorphic regions of Madagascar and highlights the preponderant role of local geological control in the distribution of natural radioactivity.

3.3. Analysis of the influence of geo-pedological characteristics and altitude on the distribution of radionuclides

To understand the factors controlling the spatial heterogeneity of the observed activity concentrations, a correlative analysis was performed by superimposing the radiological data onto the topographic and geological maps of the district. This approach allows for the deconvolution of the respective influence of altitude, lithology, and the geochemical properties of each radionuclide. The spatial distribution of ^{40}K shows a clear positive correlation with altitude, as illustrated in Fig. 8. The highest concentrations (> 278 Bq.kg^{-1}) are preferentially located on the intermediate and high-altitude flanks of the Amber Mountain volcanic massif. Conversely, the lowest values are found in the coastal plains and low-altitude plateaus. This altitudinal distribution is directly linked to the underlying geology (Fig. 9). Indeed, the high-altitude zones correspond to outcrops of more evolved volcanic rocks (trachytes, ignimbrites), which are intrinsically richer in potassium than the basalts and basanites dominant at lower altitudes. Furthermore, the more humid climatic conditions at altitude favor advanced pedogenesis, leading to the formation of deep humic soils. These soils, rich in clay-humus complexes, have a high cation exchange capacity, which promotes potassium retention, thus limiting its leaching.

International Journal of Scientific Engineering and Science
Volume 9, Issue 8, pp. 26-35, 2025. ISSN (Online): 2456-7361

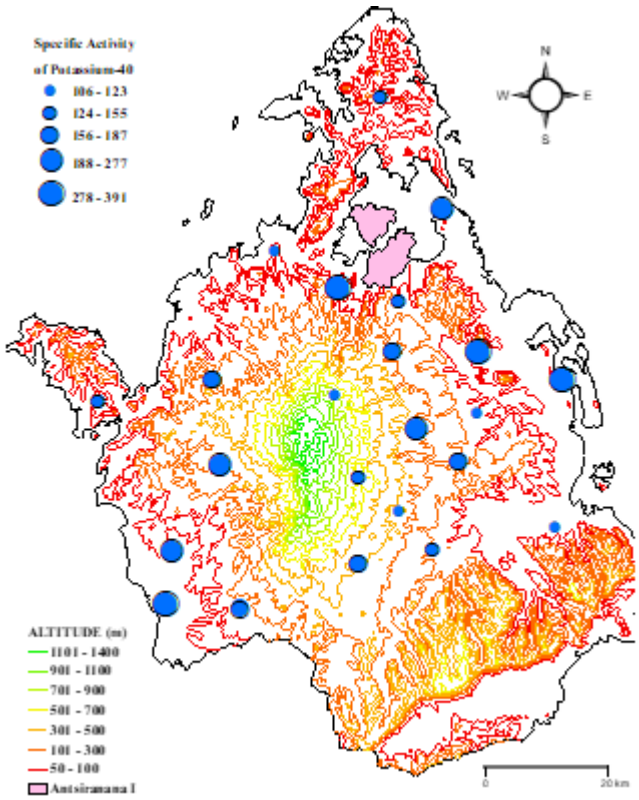

Fig. 8. Correlation between elevation and distribution of ^{40}K activity

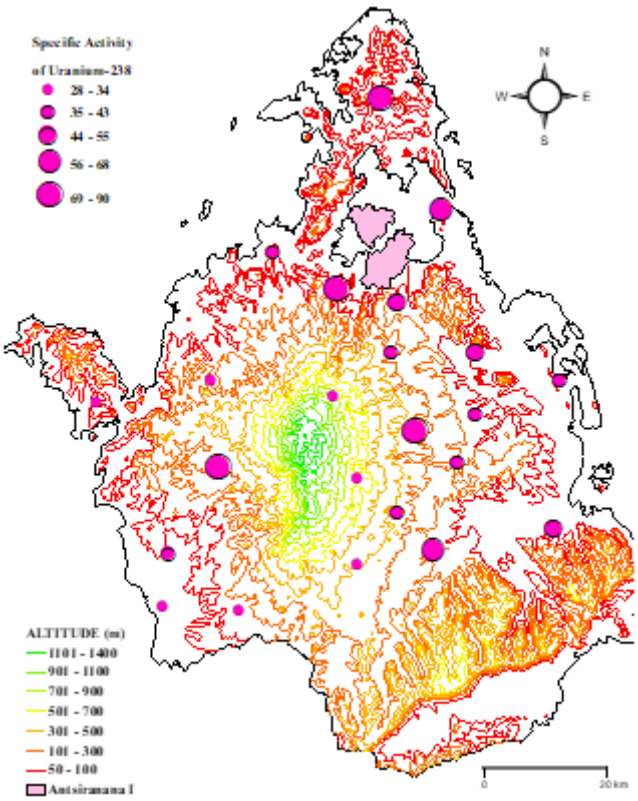

Fig. 10. Correlation between elevation and distribution of ^{238}U activity

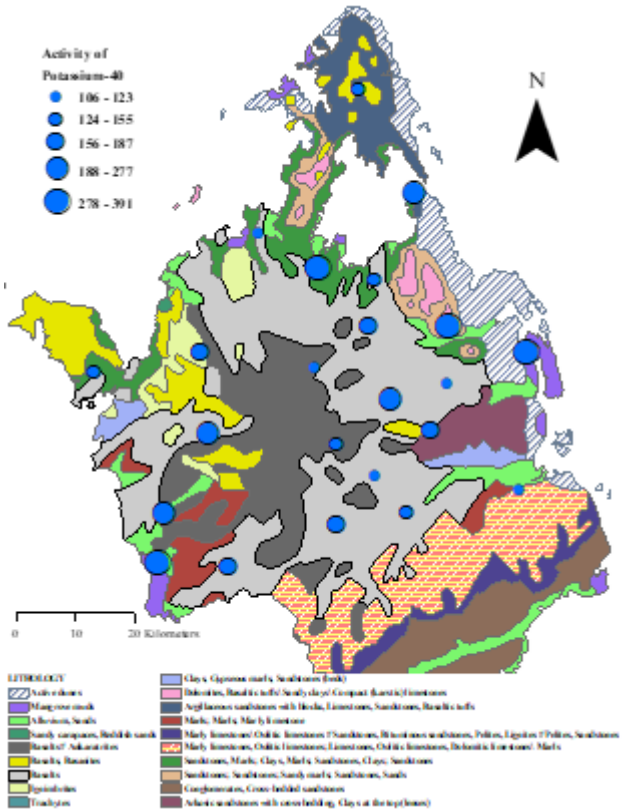

Fig. 9. Correlation between the geological formation and the distribution of ^{40}K activity

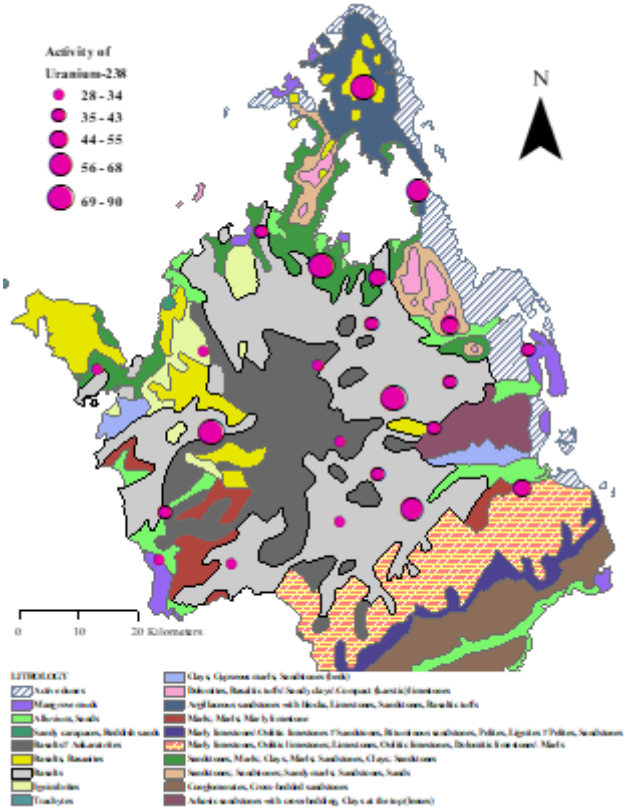

Fig. 11. Correlation between the geological formation and the distribution of ^{238}U activity

International Journal of Scientific Engineering and Science
Volume 9, Issue 8, pp. 26-35, 2025. ISSN (Online): 2456-7361

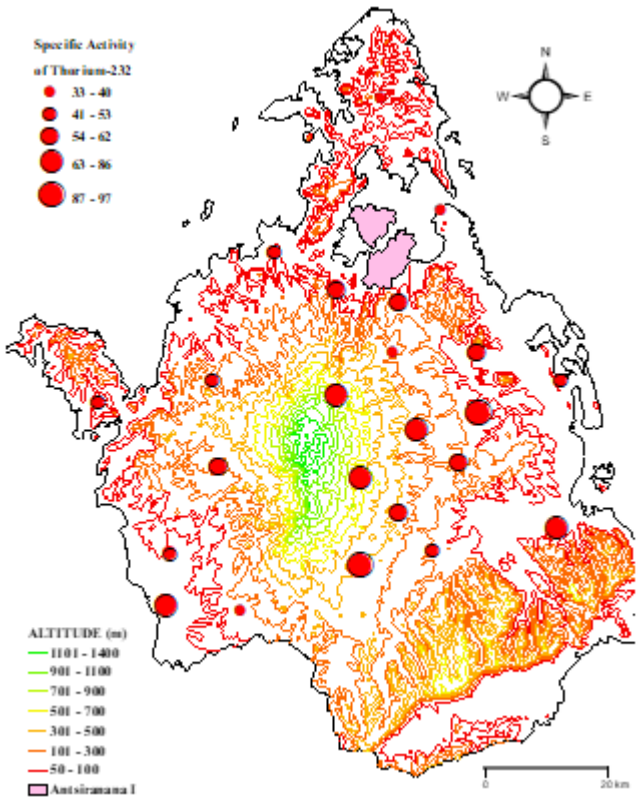

Fig. 12. Correlation between elevation and distribution of ^{232}Th activity

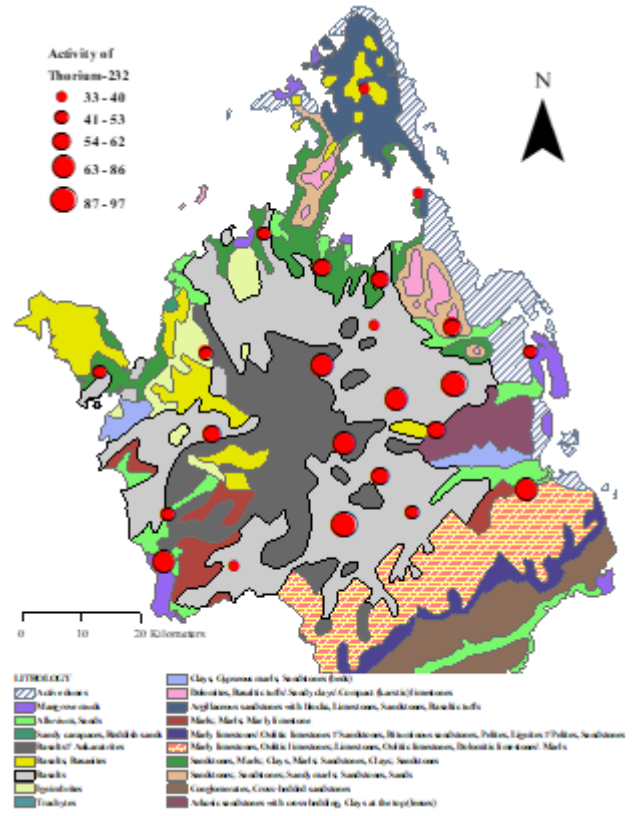

Fig. 13. Correlation between the geological formation and the distribution of ^{232}Th activity

Unlike ^{40}K, the distribution of ^{238}U shows a less direct and more complex correlation with altitude (Fig. 10). The highest concentrations (> 56 Bq.kg^{-1}) are dispersed throughout the district, found both on the volcanic massif and in the low-altitude periphery. Analysis of the correlation with the geological formation (Fig. 11) confirms this complexity, showing that the uranium hot spots are not exclusively linked to volcanic units but also overlap with peripheral sedimentary formations (marls, sandstones). This dispersion suggests a dual control. Uranium, being a relatively mobile element in oxidizing conditions, can be leached from the parent volcanic rocks and then transported by surface and groundwater before being reconcentrated in geochemical traps, such as fine clayey sediments or hydrothermal alteration zones. The distribution of ^{238}U is therefore controlled not only by the primary lithology but also significantly by secondary transport and accumulation processes.

The distribution of ^{232}Th, on the other hand, appears to be tightly governed by the nature of the parent rock. As shown in Fig. 12, there is no clear correlation between ^{232}Th concentration and altitude. In contrast, Fig. 13 shows that its spatial distribution faithfully reflects the geological map. The highest values (> 63 Bq.kg^{-1}) mainly overlap with the different volcanic units of the massif. This strong correlation is explained by the very low geochemical mobility of thorium. Its concentration in the soils is therefore a direct legacy of the composition of the source rock, likely locally enriched in heavy accessory minerals such as zircon, monazite, or apatite, which are the main carriers of thorium in magmatic rocks.

In summary, the spatial distribution of radionuclides in the district of Antsiranana II is governed by a combination of factors where lithology plays a central role, modulated by altitude (via pedogenesis) and the specific geochemical properties of each element. ^{40}K is controlled by both the type of volcanic rock (evolved vs. mafic) and altitude, which influences its retention in soils. ^{232}Th, due to its immobility, is an excellent tracer of the primary lithology. Finally, ^{238}U, being more mobile, has the most complex distribution, influenced by both the primary source and secondary geochemical redistribution processes.

IV. Conclusion

This study has established the first reference radiological map for the soils of the Antsiranana II district, filling a major gap in the environmental knowledge of northern Madagascar. The results reveal a unique geochemical signature for this volcanic region, characterized by a notable deficit in potassium (^{40}K) and a significant natural enrichment in uranium (^{238}U) and thorium (^{232}Th) compared to world averages. This profile constitutes a direct fingerprint of the volcanic substratum, which is predominantly mafic and alkaline, of the Amber Mountain.

The in-depth analysis demonstrated that the heterogeneous spatial distribution of radionuclides is governed by a complex interaction between lithology, altitude, and the specific geochemical mobility of each element. ^{40}K is controlled by both

the type of volcanic rock and altitude, which influences its retention in soils. ^{232}Th, due to its low mobility, acts as an excellent tracer of the primary lithology. Finally, ^{238}U, being more mobile, exhibits the most complex distribution, influenced not only by the primary source but also by secondary processes of leaching and reconcentration in geochemical traps.

In conclusion, this study provides not only an essential database for future environmental monitoring but also offers a valuable tool for more in-depth investigations. The collected data are fundamental for assessing risk parameters and estimating the external dose to which the rural population is exposed, thereby allowing for the evaluation of the potential radiological impact on health in a context where interaction with the soil, via agriculture, is daily. Furthermore, these results shed light on the understanding of geochemical and pedological processes in a volcanic environment and can guide land management. They constitute an indispensable reference for the sustainable management and health protection in this unique region of Madagascar.

ACKNOWLEDGMENT

The authors are deeply grateful to the teams at the Nuclear Techniques and Analysis (INSTN-Madagascar) and the Nuclear Metrology and Environment (University of Antsiranana). Their technical support and collegial collaboration were instrumental to the success of this project.

REFERENCES

[1] - UNSCEAR. Sources and effects of ionizing radiation, Vol. 1. United Nations Scientific Committee on the Effects of Atomic Radiation. Report of the General Assembly with Scientific Annexes. United Nations, New York; 2000.

[2] - M. Tzortzis, H. Tsertos, S. Christofides, G. Christodoulides. Gamma-ray measurements of naturally occurring radioactive samples from Cyprus characteristic geological rocks. Radiation Measurements, Vol. 37, Issue 3, pp. 221-229, 2003. https://doi.org/10.1016/S1350-4487(03)00028-3.

[3] - Z. Donné, M. Rasolonirina, H.C. Djaovagnono, B. Kall, N. Rabesiranana & J. Rajaobelison. Study of water radioactivity transfer from telluric origin in the Amber Mountain, Antsiranana, Madagascar. Scientific African; 13 (2021): e00902.

[4] - N. M. Demewoz, L. N. Kassie, H. G. Zeleke. Assessment of radioactivity in soil samples from Wolaita Sodo town, Ethiopia: implications for environmental and public health. Radiation Protection Dosimetry; Vol. 201, Issue 3; pp. 160–177, 2025. https://doi.org/10.1093/rpd/ncaf002

[5] - A.F. Barijaona, F. Asimanana & M. Rasolonirina. Contribution à l'étude de la radioactivité naturelle, par spectrométrie gamma, du sol dans la zone littorale d'Antalaha-Ambohitralanana Madagascar. Afrique Science, Vol. 13, No. 2, 2017.

[6] - H.C. Djaovagnono, Z. Donné, M. Rasolonirina, A.F. Solonjara & B. Kall. Spatial Distribution of Natural Radioactivity from the ^{238}U and ^{232}Th Decay Series, and ^{40}K in the Volcanic Soils of Nosy-Be Island, Madagascar. International Journal of Scientific Engineering and Science (ISSN: 2456-7361): Vol. 9, Issue 7, pp. 36-45, 2025.

[7] - M. López-Pérez, C. Martín-Luis, F. Hernández, E. Liger, J. C. Fernández-Aldecoa, J. M. Lorenzo-Salazar, J. Hernández-Armas, P. A. Salazar-Carballo. Natural and artificial gamma-emitting radionuclides in volcanic soils of the Western Canary Islands, Journal of Geochemical Exploration, Vol. 229, 2021. https://doi.org/10.1016/j.gexplo.2021.106840.

[8] - F. Ngoko, A. F. Solonjara, Z. Donné, D. Rasolozafy, and B. Kall. Étude de la radioactivité naturelle du sol : Cas du district d'Antalaha, région de SAVA, nord-est de Madagascar. American Journal of Innovative Research and Applied Sciences. Vol. 19, No 4, pp. 27-38, 2024. Doi: https://doi.org/10.5281/zenodo.13844565

[9] - F. Ngoko, Z. Donné, F. R. Randrianantenaina, D. Rasolozafy, A. F. Solonjara, and B. Kall. Assessment of the Dosimetric Impact and Radiological Risk Associated with Natural Soil Radioactivity in the Antalaha District, Madagascar. International Journal of Scientific Engineering and Science (ISSN: 2456-7361): Vol. 9, Issue 4, pp. 136-141, 2025.

[10] - B. Kall, Z. Donné, M. Rasolonirina, N. Rabesiranana & G. Rambolamanana. Contribution à l'étude de la radioactivité gamma du sable des plages de Ramena et d'Orangea, Antsiranana, Madagascar. Afrique science. Vol. 10, No. 4, pp. 23- 35, 2014.

[11] - R. R. Rakotonarivo, D. S. Ravelomanantsoa, M. Rasolonirina et F. J. Ratovonjanahary. Contribution à l'étude de la radioactivité du sol de l'extrême nord de Madagascar. American Journal of Innovative Research and Applied Sciences: Vol. 8, No.3, pp. 100-112, 2019.

[12] - Centre de Recherches, d'Etudes et d'Appui à l'Analyse Economique à Madagascar (CREAM). Monographie de la Région DIANA: pp. 1-206, 2013.

[13] - P. Ségalen. Notice sur la carte pédologique de reconnaissance au 1/200000e, feuille No. 1, Diego Suarez. Mémoires de l'Institut Scientifique de Madagascar, série D, Tome VII, 1956.

[14] - H. Besairie. Geological map, Diégo-Suarez Sheet No. 1, 1970.

[15] - P. Lemoine. Etudes géologiques dans le Nord de Madagascar : Roches éruptives basaltiques récentes, Chap. XIX, Paris, Librairie scientifique A. HERMANN, pp. 278-296, 1906.

[16] - C. Cucciniello, L. Melluso, V. Morra, M. Storey, I. Rocco, L. Franciosi, C. Grifa, C.M. Petrone and M. Vincent. New 40Ar-39Ar ages and petrogenesis of the Massif d'Ambre volcano, northern Madagascar. Volcanism and Evolution of the African Lithosphere: Geological Society of America Special Paper, Vol. 478, pp. 257–281, 2011. https://doi.org/10.1130/2011.2478(14).

[17] - C. Barat. La montagne d'Ambre (nord de Madagascar), Revue de géographie alpine. Vol. 46, No. 4, pp. 629-681, 1958.

[18] - P. Chiozzi, P. De Felice, A. Fazio, V. Pasquale, M. Verdoya. Laboratory application of NaI(Tl) γ-ray spectrometry to studies of natural radioactivity in geophysics, Applied Radiation and Isotopes, Vol. 53, Issues 1–2, pp. 127-132, 2000. https://doi.org/10.1016/S0969-8043(00)00123-8.

[19] - P. Chiozzi, V. Pasquale, M. Verdoya, S. Minato. Natural gamma-radiation in the Aeolian volcanic arc, Applied Radiation and Isotopes, Vol. 55, Issue 5, pp. 737-744, 2001. https://doi.org/10.1016/S0969-8043(01)00127-0.

[20] - G. Cinelli, L. Tositti, D. Mostacci, J. Baré. Calibration with MCNP of NaI detector for the determination of natural radioactivity levels in the field. Journal of Environmental Radioactivity; Vol. 155–156, pp. 31-37, 2016, https://doi.org/10.1016/j.jenvrad.2016.02.009.

[21] - J. E. Rahelivao, Z. Donné, A. Razafindrapata, A. I. Joelisoafara, M. Rasolonirina & B. Kall. Study of Natural Radioactivity Levels and the Associated Radiological Hazards in Soil from Ambanja City and its Surroundings, Madagascar. International Journal of Innovative Research in Science, Engineering and Technology. Vol. 12, Issue 5, 2023. DOI:10.15680/IJIRSET.2023.1202005

[22] - J. P. Stolerie, M. Rasolonirina, Z. Donné, B. Kall & N. Rabesiranana. Etude de la radioactivité naturelle d'origine tellurique du district d'Ambilobe, Madagascar. American Journal of Innovative Research Applied Sciences. Vol. 13, No. 5, pp. 518-529, 2021.

[23] - T. H. Randriamora, H. A. Razafindramiandra, Raoelina Andriambololona, S. D. Ravelomanantsoa, M. A. L. Ralaivelo, M. Rasolonirina, J. L. R. Zafimanjato, H. F. Randriantseheno. Determination of Natural Radioactivity in the North East Beach Sands of Madagascar. American Journal of Physics and Applications, Vol. 5, Issue 1, 6-12, 2017. https://doi.org/10.11648/j.ajpa.20170501.12

[24] - O. Rafidimanantsoa, M. Rasolonirina, Z. Donné, P. H. Ralaiarison, S. Tonissa, N. Rabesiranana & R. J. L. Zafimanjato. Caractérisation de la radioactivité naturelle du gisement des terres rares, de la presqu'île d'Ampasindava du nord-ouest de Madagascar. American Journal of Innovative Research Applied Sciences. Vol 13, No. 4, pp. 452-461, 2021.

[25] - A. Randrianarivo, F. Asivelo Solonjara & F. Asimanana. Contribution à l'étude de la radioactivité du sol de district de Befandriana-Nord, Madagascar. American Journal of Innovative Research and Applied Sciences. Vol. 4, No. 1, pp. 22-28, 2017.

[26] - N. Rabesiranana. Contribution à l'étude de la radioactivité environnementale à Madagascar : de la quantification à l'utilisation des traceurs radio-isotopiques environnementaux. HDR, Université d'Antananarivo, Madagascar, pp. 1-140, 2017. http://biblio.univ-antananarivo.mg/pdfs/rabesirananaNaivo1_PC_HDR_17.pdf
[27] - S. K. Anguma, V. Habakwiha & I. Habumugisha. Determination of natural radioactivity and hazards in volcanic soils of Kisoro district in south-western Uganda. Kabale University Interdisciplinary Research Journal (KURJ); Vol. 2, Issue 2; pp. 193-203; 2023.